02.72.10

1.D.2

Nuclear Physics **A183** (1972) 298—318; © *North-Holland Publishing Co., Amsterdam*

Not to be reproduced by photoprint or microfilm without written permission from the publisher

C. N. E. A. Biblioteca
ARCHIVO PUBLICACIONES
Nº 2 AÑO 1972

COLLECTIVE TREATMENT OF THE PAIRING HAMILTONIAN

(III). Numerical solutions for the $T = 1$ case

G. G. DUSSEL †, R. P. J. PERAZZO † and D. R. BÈS ††

CNEA-Ciclotron, Av. del Libertador 8250, Buenos Aires, Argentina

Received 27 October 1971

Abstract: Numerical solutions for the $T = 1$ pairing collective Hamiltonian are obtained. In the first place, the problem of the rigid rotor is solved, for any value of the asymmetry parameter Γ. Secondly, the potential energy surface due to the pairing force is constructed. A model potential, which reproduces the most important features of the pairing-force surface, is diagonalized within the basis corresponding to the six-dimensional harmonic oscillator. Thus, the properties of the collective motion can be followed from the vibrational limit to the different possible rotational limits.

1. Introduction

In paper I of this series [1]), a collective treatment of the pairing interaction between identical particles was developed and, in paper II, the description was extended to the case in which both protons and neutrons were present and interacting through a $J = 0$, charge-independent force [2]). The motivation of this series of papers is discussed in the introductions and concluding remarks of the papers I and II and will therefore not be repeated here.

In II, the collective variables were defined following the ideas of ref. [3]) and, subsequently, the transformation from the laboratory to the intrinsic system and the quantization of the kinetic energy were worked out. The general structure of the wave functions and the symmetries of the problem were discussed. The solutions for the harmonic case were outlined in order to construct the invariants of the problem.

In this paper we obtain the solutions of the collective hamiltonian derived in II for different cases. In sect. 2 we review some results which are useful for later calculations. In sect. 3 we treat the case of the rigid rotor which can be solved analytically in two extreme cases, namely when the system stabilizes around $\Gamma = 0°$ or $\Gamma = 45°$. In sect. 4 we deal with the harmonic case, since a more general situation will be solved following the same idea of ref. [11]), i.e. by diagonalizing anharmonic terms within a large but finite set of phonon states. Finally, in sect. 5 the potential energy surface arising from a pure pairing force acting between particles moving in two equally degenerate levels is considered. Due to the analytic structure of the energy surface, the actual calculations are performed for a model potential energy surface having similar properties as the corresponding pairing-force surface.

† Fellow of the Consejo Nacional de Investigaciones Cientificas y Tecnicas.
†† On leave of absence from the University of Minnesota.

We can thus follow the properties of the rotational motion as a function of the axial anisotropy, and the properties of the total collective motion from the vibrational to the different rotational limits. For the intermediate situations, we obtain values for the energies, two-body transfer matrix elements and α-transfer matrix elements. A comparison with the experimental data will be performed in a subsequent paper of this series.

2. Review

We briefly review here some properties of the Schrödinger equation corresponding to the $T = 1$ pairing collective Hamiltonian that was obtained in ref. [2]).

The six degrees of freedom of the problem are split into two groups. Four of them are the angles θ_i, ϕ specifying the orientation of the intrinsic frame in the isospin and gauge spaces. The remaining two are deformation parameters: Δ measures the total distortion of the system and Γ gives the departure from axial symmetry.

Assuming that the mass parameter B is independent of the deformation [eq. (8) ref. [2])], the Schrödinger equation reads:

$$\{T_{\rm rot}+T_{\rm vib}+T_g+T_{\theta_i,g}+V(\Delta,\Gamma)\}\Psi_{M,T,T_z}=E\Psi_{M,T,T_z}, \tag{1}$$

$$T_{\rm vib}=-\frac{1}{2B}\left\{\frac{1}{\Delta^2\sin 4\Gamma}\frac{\partial}{\partial\Gamma}\sin 4\Gamma\frac{\partial}{\partial\Gamma}+\frac{1}{\Delta^5}\frac{\partial}{\partial\Delta}\Delta^5\frac{\partial}{\partial\Delta}\right\}, \tag{2}$$

$$T_{\rm rot}+T_g+T_{\theta_i,g}=\frac{1}{2B\Delta^2}\left\{\frac{Q_x^2}{\cos^2 2\Gamma}+\frac{Q_y^2}{\cos^2\Gamma}+\frac{Q_z^2}{\sin^2\Gamma}+\frac{2\sin 2\Gamma}{\cos^2 2\Gamma}MQ_x+\frac{M^2}{\cos^2 2\Gamma}\right\}. \tag{3}$$

Here the Q_j are the angular momentum operators (in the intrinsic system) and M is the operator corresponding to the number of pairs. The eigenfunctions of this Hamiltonian have T, T_z (total isospin and its projection on the lab z-axis) and the number of pairs M as good quantum numbers. This fact, plus the symmetry properties of the Hamiltonian, allows to write the wave function as

$$\Psi_{MTT_z}(\theta_i,\phi,\Delta,\Gamma)$$
$$=\left(\frac{2T+1}{16\pi^3}\right)^{\frac{1}{2}}e^{2iM\phi}\sum_{K\geqq 0}g_K^{T,M}(\Delta,\Gamma)(1+\delta_{K,0})^{-1}(\mathscr{D}^T_{T_z,K}(\theta_i)+(-)^{T+M}\mathscr{D}^T_{T_z,-K}(\theta_i)), \tag{4}$$

where the quantum numbers associated with the motion in Δ and Γ remain yet unspecified.

The eigenfunctions (4) are orthonormalized using the volume element

$$d\tau=\tfrac{1}{4}B^5\Delta^5|\sin 4\Gamma|\,d\Omega\,d\phi\,d\Delta\,d\Gamma, \tag{5}$$

where $d\Omega$ is the volume element associated with the Euler angles in isospace. The remaining variables are defined in the intervals

$$0\leqq\phi\leqq\pi,\qquad 0\leqq\Gamma\leqq\tfrac{1}{4}\pi,\qquad 0\leqq\Delta\leqq\infty.$$

Within our scheme the operator corresponding to the two-particle transfer process is

$$\mathscr{P}_{\mu}^{\pm 1} = \pm i \mathrm{e}^{\pm 2i\phi} \Delta \left[\cos \Gamma \mathscr{D}_{\mu 0}^{1} \mp \frac{\sin \Gamma}{\sqrt{2}} (\mathscr{D}_{\mu 1}^{1} + \mathscr{D}_{\mu -1}^{1}) \right], \tag{6}$$

while the operator associated with the α-transfer is

$$S^{\pm} = \Delta^2 \mathrm{e}^{\pm 4i\phi} \cos 2\Gamma. \tag{7}$$

3. Solutions of the kinetic energy term, rigid rotor

The Hamiltonian (1) has the deformation T_{vib} and the rotational $T_{\mathrm{rot}} + T_g + T_{\theta_i, g}$ degrees of freedom formally separated. However a dynamical coupling between both motions is present since the moments of inertia that are associated with the rotations in charge and gauge spaces depend upon Δ and Γ. In a more general case even B will also depend upon Δ and Γ.

In this section we are going to neglect such coupling. Therefore, we assume that both deformation parameters are frozen at the equilibrium value Δ_0 and Γ_0. Within this framework, the functions $g_K^{T,M}(\Delta, \Gamma)$ reduce to simple constants. The limiting cases $\Gamma_0 = 0$ [refs. [4, 5])] and $\Gamma_0 = \frac{1}{4}\pi$ may be easily solved.

If $\Gamma_0 = 0$ (axial symmetry) we see from (3) that Q_z applied to the eigenfunction must give zero, i.e., only a $K = 0$ band exists. In this case eq. (4) implies that the rotational band includes states with T and M having the same parity. The energy eigenvalues, the eigenfunctions and the two-body transfer operators are, respectively

$$E_{\Gamma_0 = 0}^{M,T} = \frac{1}{2B\Delta_0^2} (T(T+1) + M^2), \tag{8}$$

$$|M, T, T_z\rangle = \left(\frac{2T+1}{16\pi^3} \right)^{\frac{1}{2}} \mathrm{e}^{2iM\phi} \mathscr{D}_{T_z, 0}^{T}(\theta_i), \tag{9}$$

$$\mathscr{P}_{\mu}^{\pm 1} = \pm i \Delta_0 \mathrm{e}^{\pm 2i\phi} \mathscr{D}_{T_z, 0}^{1}(\theta_i). \tag{10}$$

The expression (10) yields the matrix element

$$|\langle M \pm 1, T' || \mathscr{P}^{\pm 1} || M, T \rangle| = \Delta_0 \sqrt{2T+1} |\langle 1T00 | T'0 \rangle|. \tag{11}$$

The fact that there is no $\Delta T = 0$ transition implies that the reaction (τ, p) to a state of an odd nucleus with the same T as the target even-nucleus is forbidden. Thus the transition pattern is practically identical to the one arising [4, 5]) from the usual $|T_z| = 1$ pairing force. The main differences lies on the fact that the transition is now split, satisfying the triangular relations among the T's.

The four-body transfer matrix element is

$$|\langle M \pm 2, T, T_z | S^{\pm} | M, T, T_z \rangle| = \Delta_0^2. \tag{12}$$

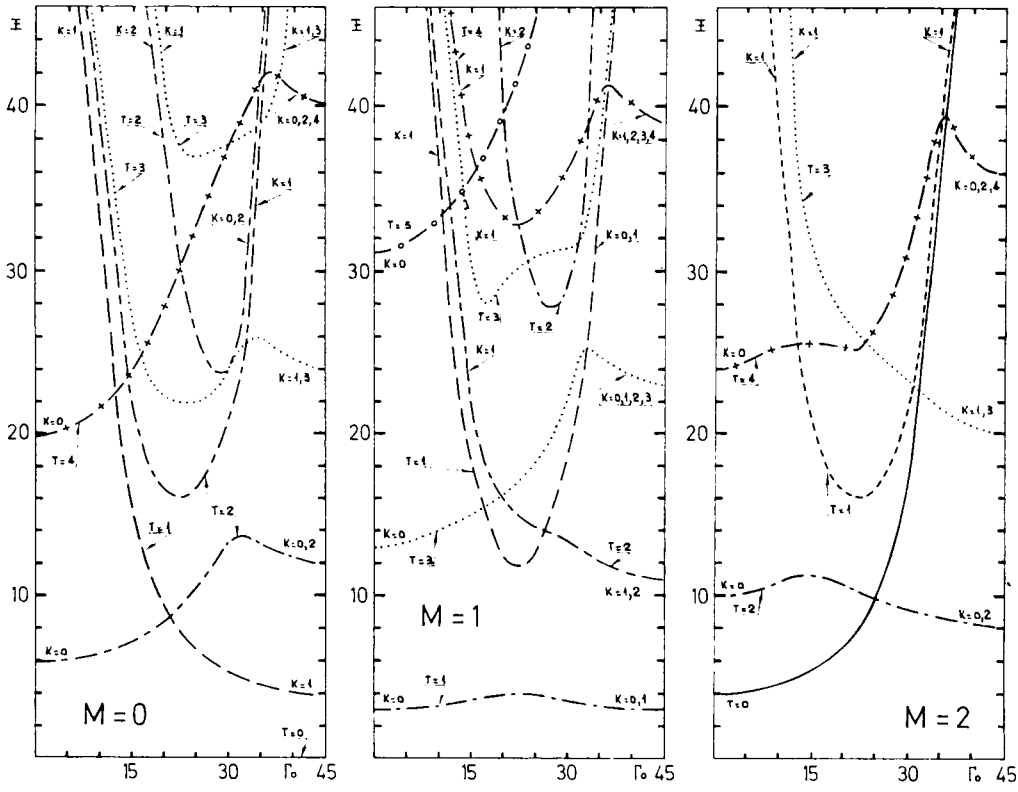

Fig. 1. Energy levels for $M \leqq 2$ and $T \leqq 5$ for the asymmetric rotor as a function of Γ_0. Energies are given in units of $2B\Delta_0$. In each case we give the K-components of the wave functions corresponding to the limits $\Gamma_0 = 0$ and $\Gamma_0 = \frac{1}{4}\pi$. If $\Gamma_0 = \frac{1}{4}\pi$ all the states of the ground state bands have projection of the isospin along the intrinsic x-axis equal to M (therefore $T \geqq M$).

The $\Gamma_0 = \frac{1}{4}\pi$ solution is obtained by requiring that the operator

$$\frac{Q_x^2 + 2\sin 2\Gamma Q_x M + M^2}{\cos^2 2\Gamma} \approx \frac{(Q_x + M)^2}{\cos^2 2\Gamma} - Q_x M, \tag{13}$$

should remain finite. This implies that the energy eigenfunctions are also eigenfunctions of Q_x with eigenvalue $-M$ and that the value of (13) is M^2. Therefore, the energies are

$$E^{T,M}_{\Gamma_0 = \frac{1}{4}\pi} = \frac{1}{2B\Delta_0^2}(M^2 + 2Q_y^2 + 2Q_z^2) = \frac{1}{B\Delta_0^2}(T(T+1) - \tfrac{1}{2}M^2), \tag{14}$$

and only the states with $T \geqq M$ subsist.

The wave functions and the pair-transfer operator are simply written if we perform a cyclic permutation of the intrinsic axis such that the new intrinsic z-axis super-

imposes with the old intrinsic x-axis. Then

$$\psi_{M,T,T_z} = \left(\frac{2T+1}{16\pi^3}\right)^{\frac{1}{2}} e^{2iM\phi} \mathscr{D}^{T}_{T_z,-M}(\theta_i), \tag{15}$$

$$\mathscr{P}^{\pm 1}_{\mu} = \Delta_0 e^{\pm 2i\phi}[\sin(\Gamma \pm \tfrac{1}{4}\pi)\mathscr{D}^{1}_{\mu,-1} - \sin(\Gamma \mp \tfrac{1}{4}\pi)\mathscr{D}^{1}_{\mu 1}], \tag{16}$$

i.e. in the new reference system, the two-body transfer operator may transfer only quasi-neutron and quasi-proton pairs. The reduced matrix elements of $\mathscr{P}^{\pm 1}_{\mu}$ are

$$|\langle M \pm 1, T' || \mathscr{P}^{\pm 1} || MT \rangle| = \Delta_0 |\langle 1, T, \pm 1, M | T', M \pm 1 \rangle| \sqrt{2T+1}. \tag{17}$$

The four-body transfer operator matrix elements vanish identically in the limit $\Gamma_0 = \frac{1}{4}\pi$.

The $T = 0$ eigenvalues of (2) can be obtained for any value of Γ_0

$$E^{T=0,M}_{\Gamma_0} = \frac{1}{2B\Delta_0^2} \frac{M^2}{\cos^2 2\Gamma_0}, \qquad M = 0, 2, \ldots, \tag{18}$$

which says that the energy goes to ∞ as $\Gamma_0 \to \frac{1}{4}\pi$. This is consistent with the fact that the only states which survive are those with $T \geqq M$, in this limit. For any other values of T, eq. (15) can be numerically solved. The energy eigenvalues for $T \leqq 5$ and $M = 0$, 1, 2 are given in fig. 1. The previously discussed features of $\Gamma_0 = 0$ and $\Gamma_0 = \frac{1}{4}\pi$ are reproduced. In addition, it is worthwhile to mention the fact that in the vicinity of $\Gamma_0 = 23°$–$25°$ there is a doublet of excited states with $T = 1, 2$ for $M = 0$, a low $T = 1$ and an excited triplet $T = 1, 2, 3$ for $M = 1$, and a low doublet $T = 0, 2$ for $M = 2$. This spectrum resembles the one corresponding to the vibrational limit [refs. [4, 6, 5])] but for the absence of a $T = 0$ excited state if $M = 0$ and for the existence of only one excited $T = 1$ state for $M = 1$.

The two-body transfer matrix elements show also a great similarity with the vibrational scheme in the neighbourhood of 25° since the transitions $(M, T) \leftrightarrow (M', T') = (0, 0) \leftrightarrow (1, 1)$, $(0, 1) \leftrightarrow (1, 1)$, $(0, 2) \leftrightarrow (1, 1)$ are predicted to be of the same order of magnitude, while the $(0, 2) \leftrightarrow (1, 3)$ should be somewhat stronger [see fig. 2 and refs. [5, 6])].

The four-particle transfer matrix elements continuously decrease from $\Gamma_0 = 0$ to $\Gamma_0 = \frac{1}{4}\pi$. Higher T's are seen to be hindered faster than lower T's as a function of Γ_0. This hindrance may be understood in the following way: in the rotational limit the four-body transfer can also be calculated as the product of the two-particle transfer matrix elements connecting the states with $M = 0$ and 1 times those connecting $M = 1$ and 2. In spite of the fact that for $\Gamma_0 = \frac{1}{4}\pi$ the first ones are enhanced, the second ones are very hindered, since the $T = 0$, $M = 2$ state is forbidden because of symmetry conditions of the wave functions (see fig. 1).

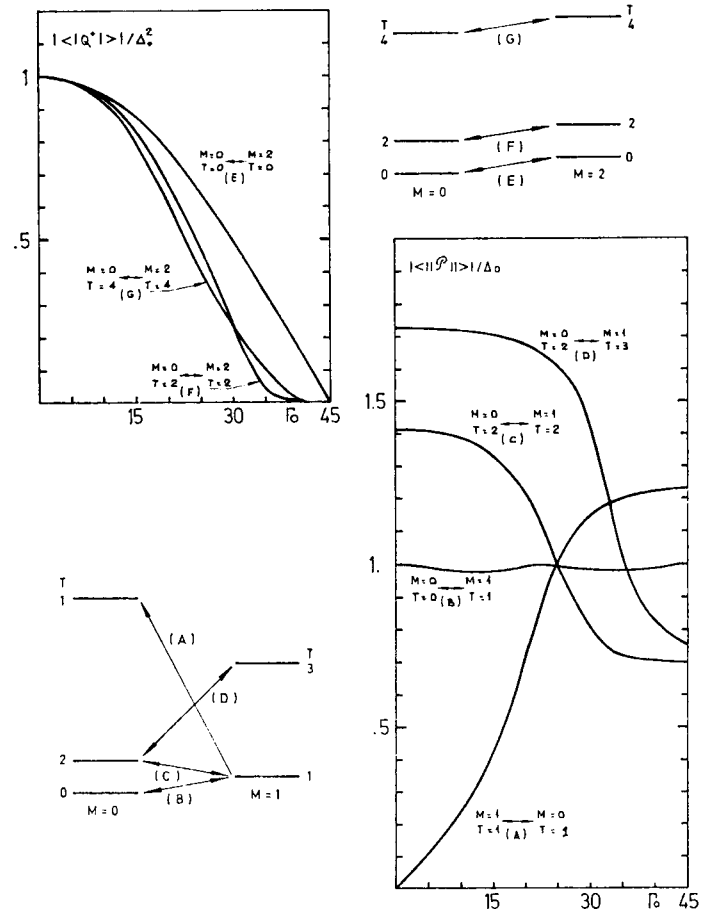

Fig. 2. Upper part: Absolute value of the α-transfer matrix elements in units of Δ_0^2. A level scheme to the right clarifies the transitions that are plotted as a function of Γ_0. Lower part: Absolute value of the two-particle transfer matrix elements in units of Δ_0. A level scheme to the left shows the transitions that are plotted as a function of Γ_0.

4. The Γ-independent potential energy surfaces

If

$$V(\Delta, \Gamma) = V(\Delta), \tag{19}$$

the coefficients $g_K^{T,M}(\Delta, \Gamma)$ in (4) may be factorized

$$g_K^{T,M}(\Delta, \Gamma) = \mathscr{R}_{n,\lambda}^{T,M}(\Delta) g_K^{M,T,\lambda}(\Gamma), \tag{20}$$

where the two quantum numbers, n, λ, correspond to the number of nodes of the radial part of the wave function and to the seniority respectively. The radial part $\mathscr{R}_{m,\lambda}^{T,M}(\Delta)$

is the solution of the differential equation

$$\left\{-\frac{1}{2B}\frac{1}{\Delta^5}\frac{\partial}{\partial\Delta}\Delta^5\frac{\partial}{\partial\Delta}+\frac{\lambda(\lambda+4)}{2B\Delta^2}+V(\Delta)-E\right\}\mathscr{R}^{T,M}_{n,\lambda}(\Delta)=0. \tag{21}$$

For the particular case of the harmonic oscillator $V=\frac{1}{2}C\Delta^2$, it is given by

$$\mathscr{R}^{T,M}_{n,\lambda}(\Delta)=\mathscr{N}_{n,\lambda}\rho^{\lambda}e^{-\frac{1}{2}\rho^2}L_n^{\lambda+2}(\rho^2),\qquad \rho=\sqrt{\frac{C}{\omega}}\,\Delta, \tag{22}$$

$$\mathscr{N}_{n,\lambda}=\left[\frac{2(n!)}{[(n+\lambda+2)!]^3}\left(\frac{C}{\omega}\right)^3\right]^{\frac{1}{2}},\qquad \omega=\sqrt{\frac{C}{B}}, \tag{23}$$

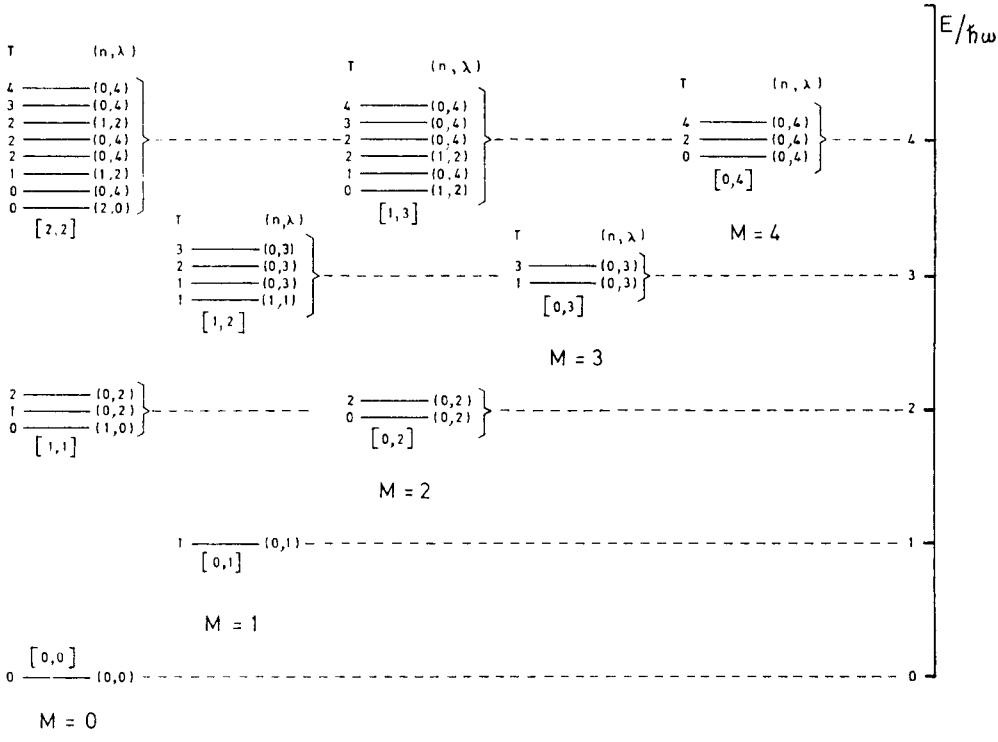

Fig. 3. Energy spectrum for the harmonic case. All levels that are grouped by a bracket have the same energy but are split in order to display the quantum numbers that are associated with each one. Under each group is given (n_r, n_a) i.e. the number of removal and addition phonons corresponding to each case. The zero-point energy has been removed.

and the $L_n^{\lambda+2}(\rho^2)$ are the generalized Laguerre polynomials [7]). The energies are given by

$$E_{n,\lambda}=(2n+\lambda+3)\omega, \tag{24}$$

(see fig. 3). Each time that n is increased by one, for a given value of λ, a pair of phonons coupled to total isospin 0 is added and a Δ-band is built.

The equation for the remaining variables reads

$$\left[-\frac{1}{\sin 4\Gamma}\frac{\partial}{\partial\Gamma}\sin 4\Gamma\frac{\partial}{\partial\Gamma}+\frac{Q_x^2}{\cos^2 2\Gamma}+\frac{Q_y^2}{\sin^2\Gamma}+\frac{Q_z^2}{\cos^2\Gamma}\right.$$
$$\left.+\frac{\sin 2\Gamma}{\cos^2 2\Gamma}2MQ_x+\frac{M^2}{\cos^2 2\Gamma}-\lambda(\lambda+4)\right]\Phi_{T_z}^{T,M,\lambda}(\Gamma,\phi,\theta_i)=0. \quad (25)$$

The procedure to obtain the functions $\Phi_{T_z}^{T,M,\lambda}$ is outlined in ref. [2]) and follows the same method as the one applied to the quadrupole case in ref. [8]). First a basic set of tensors $Z_{T_z}^{T,m}(\Gamma,\phi,\theta_i)$ is constructed. This set is given in appendix 1 of ref. [2]) for $T\leqq 2$. The solutions of (25) may be expressed as linear combinations of this basic set with coefficients that are polynomials in $x=\cos 2\Gamma$, with a definite parity in the variable x.

$$\Phi_{T_z}^{T,M,\lambda}=\frac{e^{2iM\phi}}{\sqrt{\pi}}\sum_m f_m^{T,\lambda}(x)e^{-2im\phi}Z_{T_z}^{T,m}(\Gamma,\phi,\theta_i). \quad (26)$$

The coupled system of differential equations determining the $f_m^{T,\lambda}(x)$ has either dimensions T or $T+1$, according to the parity of M. Recurrence relations for the coefficients in the polynomials $f_m^{T,\lambda}(x)$ are obtained in the appendix 1 for $T\leqq 2$. By using (25) and (26) a close relationship can be worked out between the $g_K^{M,T,\lambda}$ and the $f_m^{T,\lambda}$. The two-body transfer operator has reduced matrix elements given by

$$\langle n,\lambda,M\pm1,T||\mathscr{P}^{\pm1}||n',\lambda+1,M,T'\rangle=\pm2i\left(\frac{\omega}{C}\right)^{\frac{1}{2}}\sqrt{2T'+1}\langle n,\lambda|\rho|n',\lambda+1\rangle$$
$$\times\sum_{\substack{K\geqq 0\\K'\geqq 0}}(1+\delta_{K,0})^{-1}(1+\delta_{K',0})^{-1}\int_0^{\frac{1}{4}\pi}g_K^{T,M\pm1,\lambda^*}g_{K'}^{T,M,\lambda+1}$$
$$\times\left(\cos\Gamma A_{KK'}^{T,T',M}\mp\frac{\sin\Gamma}{\sqrt{2}}B_{KK'}^{T,T',M}\right)\sin 4\Gamma\,d\Gamma, \quad (27)$$

with

$$\langle n,\lambda|\rho|n-1,\lambda+1\rangle=-\sqrt{n},\qquad \langle n,\lambda|\rho|n,\lambda+1\rangle=\sqrt{\lambda+n+3}, \quad (28)$$

$$A_{KK'}^{T,T',M}=\langle 1T'0K'|TK\rangle+(-)^{T'+M}\langle 1T'0-K'|TK\rangle,$$

$$B_{KK'}^{T,T',M}=(\langle 1T'1K'|TK\rangle+\langle 1T'-1K'|TK\rangle)$$
$$+(-)^{T+M+1}(\langle 1T1K'|T-K\rangle+\langle 1T'-1K'|T-K\rangle). \quad (29)$$

Within this scheme the matrix element of the operator associated with the α-transfer is

$$\langle n,\lambda,M\pm2,T,T_z|S^{\pm}|n',\lambda',M,T,T_z\rangle$$
$$=\left(\frac{\omega}{C}\right)\langle n,\lambda|\rho^2|n',\lambda'\rangle\sum_K\int_0^{\frac{1}{4}\pi}g_K^{M+2,T,\lambda^*}g_K^{M,T,\lambda}\cos 2\Gamma\sin 4\Gamma\,d\Gamma. \quad (30)$$

The matrix elements of powers of Δ and $\cos 2\Gamma$ are in principle easy to compute since they may be reduced to sums of integrals of the form $\int e^{-\rho^2}\rho^n d\rho$ and $\int x^n dx$ respectively.

5. The pairing-force potential energy surface

The potential energy surface associated with the $T = 1$ pairing force can be obtained in the same way as in ref. [1]) using as an intrinsic system the one defined in ref. [9]), in which quasi-protons and quasi-neutrons are uncoupled. Within this framework the two deformation parameters Δ_n and Δ_p are related to Δ and Γ by

$$\Delta_n = \Delta \cos(\Gamma + \tfrac{1}{4}\pi),$$

$$\Delta_p = \Delta \sin(\Gamma + \tfrac{1}{4}\pi), \tag{31}$$

therefore

$$V_{pair}(\Delta, \Gamma) = V_{pair}(\Delta_n, \Delta_p) = V_0(\Delta_n) + V_0(\Delta_p), \tag{32}$$

$$V_0(\Delta_\tau) = \langle\tilde{0}|H_{s.p.}|\tilde{0}\rangle + \langle\tilde{0}|H_{pair}|\tilde{0}\rangle$$

$$= \sum_j \Omega_j \varepsilon_j - \sum_j \Omega_j \varepsilon_j^2 (\varepsilon_j^2 + \Delta_\tau^2)^{-\frac{1}{2}} - \tfrac{1}{4}G\Delta_\tau^2 \Big(\sum_j \Omega_j (\varepsilon_j^2 + \Delta_\tau^2)^{-\frac{1}{2}}\Big)^2, \tag{33}$$

in eq. (33) $|\tilde{0}\rangle$ denotes the BCS vacuum for both quasi-protons and quasi-neutrons and Δ_τ denotes either Δ_n or Δ_p

$$|\tilde{0}\rangle = \prod_{jm\tau} (u_{j\tau} + v_{j\tau} a^\dagger_{jm\tau} a^\dagger_{\widetilde{jm\tau}})|0\rangle, \qquad \tau = 1, -\tfrac{1}{2}. \tag{34}$$

Here, $a^+_{jm\tau}$ creates a quasi-nucleon in a quantum state j, m with isobaric spin projection τ. The label $\widetilde{j, m, \tau}$ denotes the time reversed state of j, m, τ. When (33) is used for the case of two equally degenerate j-shells, separated by a distance 2ε, one gets

$$\frac{1}{2\Omega\varepsilon} V_{pair}(\Delta, \Gamma) = 2 - \left\{\frac{\varepsilon}{[\varepsilon^2 + \Delta^2 \cos^2(\Gamma + \frac{1}{4}\pi)]^{\frac{1}{2}}} + \frac{X}{2} \frac{\Delta^2 \cos^2(\Gamma + \frac{1}{4}\pi)}{\varepsilon^2 + \Delta^2 \cos^2(\Gamma + \frac{1}{4}\pi)}\right\}$$

$$- \left\{\frac{\varepsilon}{[\varepsilon^2 + \Delta^2 \sin^2(\Gamma + \frac{1}{4}\pi)]^{\frac{1}{2}}} + \frac{X}{2} \frac{\Delta^2 \sin^2(\Gamma + \frac{1}{4}\pi)}{\varepsilon^2 + \Delta^2 \sin^2(\Gamma + \frac{1}{4}\pi)}\right\}. \tag{35}$$

In (35) the dimensionless parameter $X = \Omega G/\varepsilon = G/G_C$ is such that for $X = 1$ the pairing phase transition takes place.

The contour plots of (35) are shown in fig. 4. The gradient of (35) can easily be studied by using (32). The first derivatives of $V(\Delta_\tau)$ vanish at $\Delta_\tau = 0$ and $\Delta_\tau^2 = \varepsilon^2$

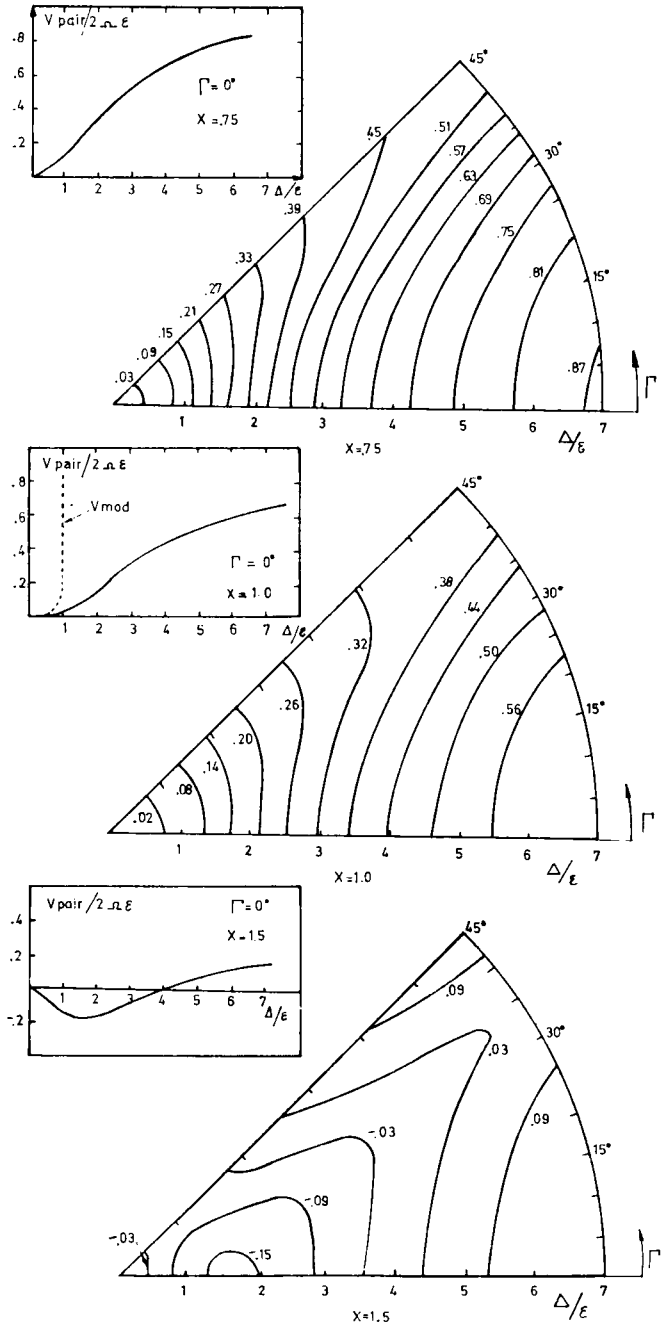

Fig. 4. Contour plots of the $T = 1$ pairing potential energy surface in units of $2\Omega\varepsilon$ for a symmetric two-level model. The phase transition takes place for $X = 1$. At the left of each plot is shown the behaviour of V_{pair} as a function of Δ/ε for $\Gamma = 0$. The gradient from one contour line to the next is kept constant in the three plots. For $X > 1$ a minimum is located outside the origin, therefore showing a permanent distortion of the system.

(X^2-1). By further analysis of the second derivative † it is possible to obtain the extremal points

$$\begin{aligned} &\Delta_n = \Delta_p = \Delta = 0 && \text{minimum if } X < 1, \\ &\Delta_n = \Delta_p = \Delta = 0 && \text{maximum if } X > 1, \\ &\Delta_n^2 = \Delta_p^2 = \tfrac{1}{2}\Delta^2 = \varepsilon^2(X^2-1), \qquad \Gamma = 0 && \text{minimum if } X > 1. \end{aligned} \tag{36}$$

All other possibilities are saddle points.

The pairing-potential energy-surface is a particular case of a more general one, which should satisfy the requirements of being invariant under rotations in both isospin and gauge spaces. This in turn implies that an arbitrary potential can be expanded in integral powers of Δ^2 and $\Delta^4 \cos^2 2\Gamma$. Therefore these quantities are analogous to β^2 and $\beta^3 \cos 3\gamma$, respectively, of the quadrupole case.

Therefore a general expansion is

$$V(\Delta, \Gamma) = \sum_{l=0}^{\infty} V_{2l} \Delta^{2l} \Big(\sum_{s=0}^{m} k_{s,l} \cos^{2s} 2\Gamma \Big),$$

$$m = \begin{cases} \tfrac{1}{2}l & \text{if } l \text{ is even}, \\ \tfrac{1}{2}(l-1) & \text{if } l \text{ is odd}. \end{cases} \tag{37}$$

In order to deal with (37), the same method of ref. [11]) can be followed. At the end of the previous section, we have indicated how to construct the matrix elements of each term in (37) within the harmonic oscillator basis.

A series expansion of (35) can indeed be brought into the form (37). If, however, a diagonalization is attempted of a truncated expansion, the results are poor since the

† The values of the second derivative are related to the frequencies ω_Δ and ω_Γ through

$$\omega_\Delta = \left[\frac{1}{B_\Delta} \left(\frac{\partial^2 V_{\text{pair}}(\Delta, \Gamma)}{\partial \Delta^2} \right)_{\substack{\Delta_{\min} \\ \Gamma_{\min}}} \right]^{\frac{1}{2}}, \qquad \omega_\Gamma = \left[\frac{1}{B_\Gamma} \left(\frac{1}{\Delta^2} \frac{\partial^2 V_{\text{pair}}(\Delta, \Gamma)}{\partial^2 \Gamma^2} \right)_{\substack{\Delta_{\min} \\ \Gamma_{\min}}} \right]^{\frac{1}{2}},$$

where B_Δ and B_Γ are the inertial parameters associated with the Δ and Γ motions. These can be obtained using the cranking model prescription and are found to be

$$B_\Delta = B_n \cos^2(\Gamma + \tfrac{1}{4}\pi) + B_p \sin^2(\Gamma + \tfrac{1}{4}\pi), \qquad B_\Gamma = B_n \sin^2(\Gamma + \tfrac{1}{4}\pi) + B_p \cos^2(\Gamma + \tfrac{1}{4}\pi),$$

$$B_n = \frac{\Omega\varepsilon^2}{[\varepsilon^2 + \Delta^2 \cos^2(\Gamma + \tfrac{1}{4}\pi)]^{\frac{1}{2}}}, \qquad B_p = \frac{\Omega\varepsilon^2}{[\varepsilon^2 + \Delta^2 \sin^2(\Gamma + \tfrac{1}{4}\pi)]^{\frac{1}{2}}},$$

therefore one gets

$$\begin{aligned} &X < 1 \text{ (minimum at } \Delta_n = \Delta_p = 0), && \omega_\Delta = 2\varepsilon\sqrt{1-X}, \\ &X > 1 \text{ (minimum at } \Delta_n = \Delta_p = \varepsilon\sqrt{X^2-1}), && \omega_\Delta = \omega_\Gamma = 2\varepsilon\sqrt{X^2-1}. \end{aligned}$$

These results can also be checked within the RPA approximation [5]) or in an exact calculation [10]).

expansion of $V_{\text{pair}}(\Delta, \Gamma)$ is of alternating signs and very slow convergence (a truncated series expansion in general behaves improperly at infinity).

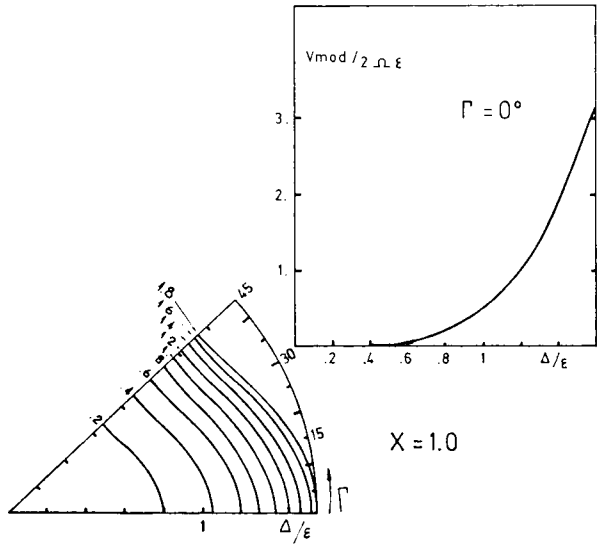

Fig. 5. Contour plot of V_{mod} for $X = 1$. In this plot $\beta = \frac{1}{2}$, $\varepsilon = 1$ and $\Omega = 10$.

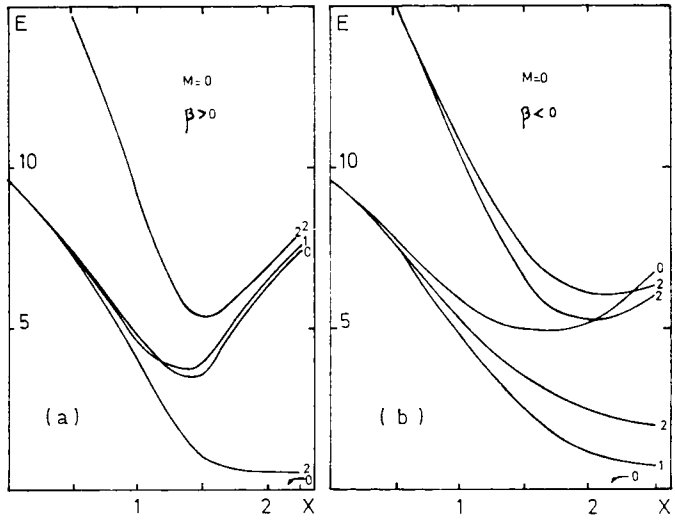

Fig. 6. Low-energy levels with $M = 0$ and $T \leqq 2$, obtained with V_{mod}, as a function of X: In (a) V_{mod} is chosen to stabilize around $\Gamma = 0$; in (b) the minimum is instead located at $\Gamma = \frac{1}{4}\pi$.

We have performed some numerical calculations with a model potential energy surface

$$V_{\text{mod}}(\Delta, \Gamma) = 2\Omega\varepsilon \left[\alpha(1-X)\frac{\Delta^2}{\varepsilon^2} + X\frac{\Delta^4}{\varepsilon^4}(1-\beta\cos^2 2\Gamma) \right], \tag{38}$$

that behaves in a similar fashion as (35), having a phase transition from spherical to deformed for $X = 1$ (at that point the harmonic frequency tends to zero). A qualitative agreement is therefore to be expected with the pairing result for values of X that are close to the transition region. If $\beta = \frac{1}{2}$ and $X > 1$, then $\omega_\Delta = \omega_\Gamma$, therefore reproducing another feature of the potential (35). The parameter α helps to produce smooth or sudden phase transitions according to whether high or low values are chosen for it.

In addition, if β is chosen to be negative, the effects of a minimum at $\Gamma = \frac{1}{4}\pi$ can be investigated.

The contour plots of V_{mod}, for $X = 1$, are given in fig. 5. If compared with the corresponding plot of fig. 4, the potential is seen to grow much faster due to the fact that the term in Δ^4 is not partially cancelled by higher-order terms.

The potential (38) has been diagonalized in the basis of all states up to 20 phonons for the cases $M = 0$, $T = 0, 1, 2$; $M = 1$, $T = 1, 2$ and $M = 2$, $T = 0$. In all these calculations, the parameters where fixed at $\alpha = 3.0$, $\Omega = 10$, $\varepsilon = 1$ and $\beta = \pm\frac{1}{2}$.

In addition, the inertial parameter B was chosen to be $\Omega/2\varepsilon^3$, as in the pairing vibrational limit. It must be borne in mind that in the pairing case, B is also a function of Δ and Γ. Therefore, a strict comparison of V_{mod} and H_{pair} is in principle not achieved.

In fig. 6 the lowest energy levels for $M = 0$ are plotted as a function of the parameter X. The left part of it shows the effect of a phase transition of the pairing type in which the minimum of the potential energy surface is found at $\Gamma = 0°$ for all values of $X > 1$. In the rotational limit, a band is built on top of the ground state having only even-T states. The Δ-vibrational band ($T = 0, 2$) appears degenerate † with the Γ-vibration ($T = 1, 2$). These features are consistent with the results obtained in exact calculations [10]).

In the right part of fig. 6, β is chosen negative. In this case, the equilibrium position is located at $\Gamma = \frac{1}{4}\pi$. The structure of the ground state band has changed, having the same features that were obtained in sect. 3 for the rigid rotor (see fig. 1). For both $\beta \gtrless 0$, the two-phonon, $T = 0$ state becomes a member of a Δ-vibrational band. As expected, both cases ($\beta \gtrless 0$) do not differ drastically from each other if $X < 1$.

In addition to energy eigenvalues, two- and four-particle transfer matrix elements are calculated. In fig. 7, the transitions connecting states with $M = 0$ and $M = 1$ are plotted as a function of X. The dotted lines correspond to $\beta < 0$ and the full lines to $\beta > 0$ (pairing-like potential energy surface).

Again a general qualitative agreement is found with known pairing results [1, 10]). The population of the first excited $T = 0$ state tends to zero for large values of X. This is consistent with the fact that, in that limit, the intrinsic structure of this state differs from that of the ground state with $M = 1$. In the pairing-like case, the same happens with the state with $T = 1$ and $M = 0$. For $\beta < 0$, this no longer holds since the $T = 1$ state of $M = 0$ is a member of the ground state rotational band, therefore having the

† See footnote on previous page.

same intrinsic structure as the state with $M = 1$ and $T = 1$. The two-particle transfer therefore behaves in a similar fashion as the one populating the $T = 0$ state. In the rotational limit this two matrix elements are found to be in the same ratio as the corresponding Clebsch-Gordan coefficients. All these features are also consistent with the results obtained in sect. 3 (see fig. 2).

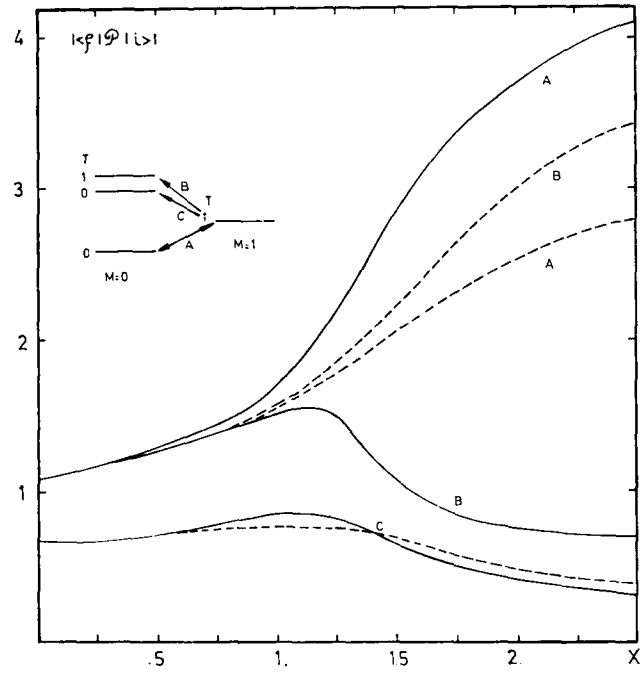

Fig. 7. Two-particle transfer matrix elements connecting $M = 0$ with $M = 1$ states. To the left a level scheme clarifies the transitions that are considered. Full lines correspond to the same case as to the left of fig. 6 (the minimum of V_{mod} is at $\Gamma = 0$) and the dotted lines to the same case as to the right of fig. 6 (V_{mod} stabilizes at $\Gamma = \frac{1}{4}\pi$).

In fig. 8, the four-body transfer matrix elements are plotted. The ground state to ground state transition for $\beta > 0$ again shows a qualitative agreement with exact calculations [12]). When $\beta < 0$ the corresponding transition is hindered as shown in fig. 2.

As an illustration of the possible deformations of the system, we have plotted in fig. 9 the probability distribution for the ground state and first A-vibrational state ($X = 1.75$).

6. Conclusions

In this paper the adiabatic treatment of the $T = 1$ pairing Hamiltonian is used in order to investigate the dynamical coupling of rotations and vibrations in isospin and gauge spaces.

This is done following the lines of ref. [2]) where four collective (rotational) variables and two intrinsic (deformation) parameters are defined. The solutions of the six dimensional harmonic oscillator are obtained within this framework. These are used as a complete basis within which a general potential can be diagonalized.

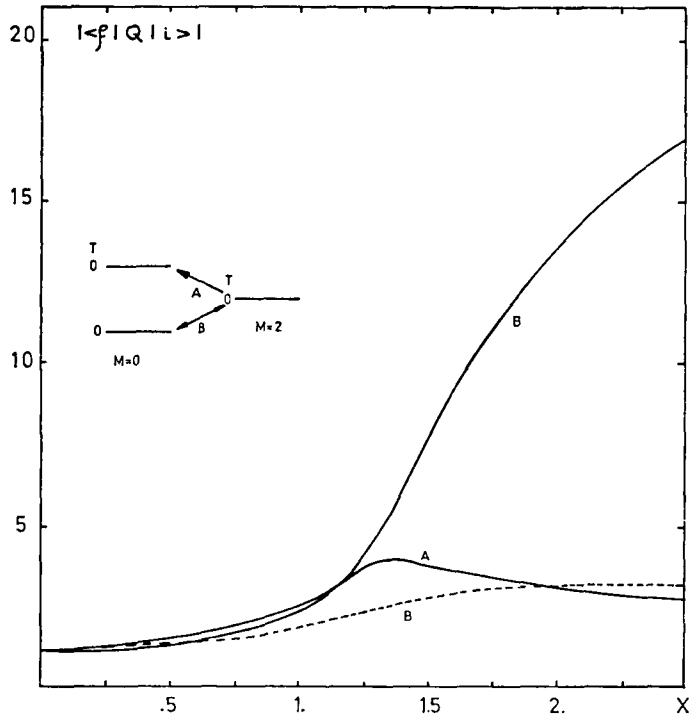

Fig. 8. Four-particle transfer matrix elements connecting the $T = 0$ states of $M = 0$ and 2. To the left, a level scheme shows the transitions that are considered. Full lines are obtained with V_{mod} stabilizing at 0° while the corresponding dotted line is obtained with V_{mod} stabilizing at $\frac{1}{4}\pi$.

An alternative way of building the basic set of phonon states is to use two uncoupled three dimensional harmonic oscillators that are associated with the addition and removal modes. This other scheme may still be the most convenient one to use if the anharmonicities are small [13]).

The advantage of the present scheme is that the equilibrium values of the intrinsic variables in a deformed case are related to the gap parameters that are provided by the BCS treatment.

The limiting case of a rigid asymmetric rotor is discussed. The solutions for $\Gamma = 0$ and $\Gamma = \frac{1}{4}\pi$ correspond to axially symmetric rotators. However the structure of the rotational bands is different in each limit. In the first case all states have $K = 0$ and all T's of the same parity of M are allowed. In the second, there are present all T's that satisfy $T \geqq M$. In addition in this latter case the four-particle transfer is forbidden.

The Δ and Γ dynamics is studied diagonalizing a model Hamiltonian. The phase transition is properly described and the results are in qualitative agreement with previous exact calculations. Furthermore this collective description may enable us to deal with other residual forces acting in the channel with $J = 0$ and $T = 1$, and causing the system to stabilize, for instance, at $\Gamma \neq 0$.

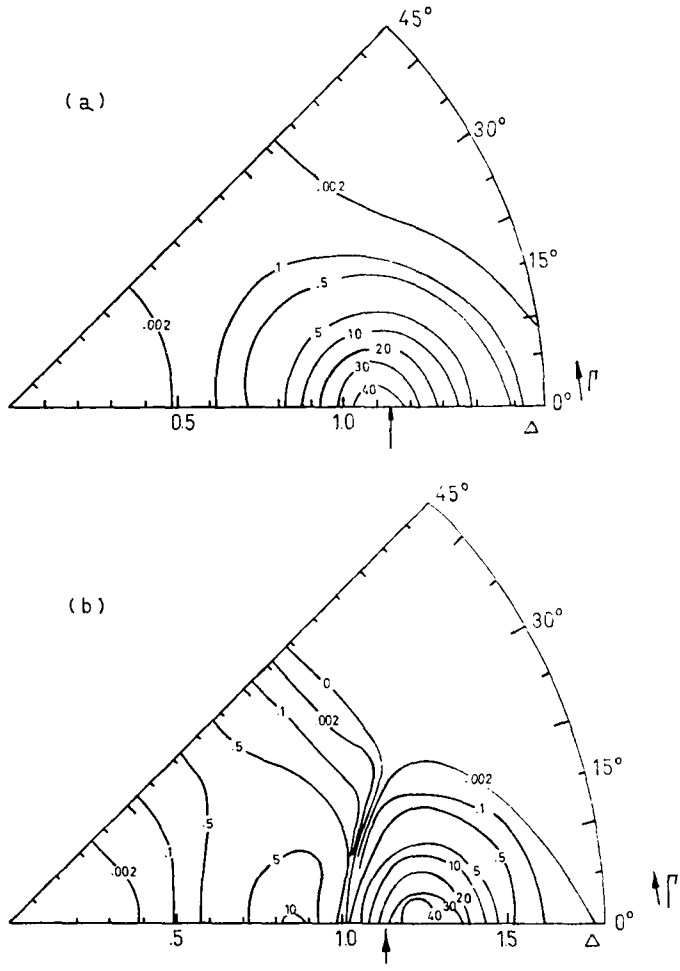

Fig. 9. Contour plots of the probability distribution. The plots are obtained using the model potential corresponding to fig. 6 (a) with $X = 1.75$. Graph (a) represents the ground state and (b) the first excited state (Δ-vibration). The arrows indicate the equilibrium value of Δ.

Discussions with Profs. A. Bohr and B. Mottelson and with Drs. R. A. Broglia, O. Hansen, E. Maqueda, O. Nathan and B. Sørensen are very gratefully acknowledged. The financial support of the Fundación Juan Bautista Sauberan is very much appreciated.

Appendix

SOLUTION OF THE Γ-DEPENDENT PART OF THE WAVE FUNCTION

$T = 0$. The general solution is written

$$\Phi_0^{0,M,\lambda} = \frac{e^{2iM\phi}}{\sqrt{\pi}} f_0^{0,\lambda}(\cos 2\Gamma), \tag{A.1}$$

where $f_0^{0,\lambda}(x)$ satisfies the equation

$$\left\{(1-x^2)\frac{d^2}{dx^2} + \frac{1}{x}(1-3x^2)\frac{d}{dx} - \frac{M^2}{4x^2} + \tfrac{1}{4}\lambda(\lambda+4)\right\} f_0^{0,\lambda}(x) = 0. \tag{A.2}$$

Throughout this appendix $x = \cos 2\Gamma$. The solution of (A.2) is:

$$f_0^{0,\lambda}(x) = x^{\frac{1}{2}|M|} \sum_{n=0}^{n_{max}} a_n x^n. \tag{A.3}$$

The coefficients in (A.3) are defined by the recurrence relation

$$a_{n+2} = -\frac{4\eta_0^n a_n}{(2n+M+4)^2 - M^2}, \tag{A.4}$$

where

$$\eta_\alpha^n = \tfrac{1}{4}\{\lambda(\lambda+4) - (2n+M+\alpha)(2n+M+\alpha+4)\}, \tag{A.5}$$

and $n_{max} = \frac{1}{2}(\lambda - M)$ with λ and M even. The overlap integral is

$$\int_0^1 f_0^{0,\lambda}(x) f_0^{0,\lambda'}(x) x\,dx = \mathcal{N}_\lambda \delta_{\lambda,\lambda'}, \tag{A.6}$$

$T = 1$, *M even.* The general solution is written:

$$\Phi_{T_z}^{1,M,\lambda}(\Gamma, \phi, \theta_i) = f_0^{1,\lambda}(x)\tfrac{1}{2}\sin 2\Gamma\{\mathscr{D}^1_{T_z,1}(\theta_i) - \mathscr{D}^1_{T_z,-1}(\theta_i)\}\frac{e^{2iM\phi}}{\sqrt{\pi}}, \tag{A.7}$$

where $f_0^{1,\lambda}(x)$ satisfies the equation

$$\left\{(1-x^2)\frac{d^2}{dx^2} + \frac{1}{x}(1-5x^2)\frac{d}{dx} - \frac{M^2}{4x^2} + \tfrac{1}{4}\lambda(\lambda+4) - 3\right\} f_0^{1,\lambda}(x) = 0. \tag{A.8}$$

The solution of (A.8) is

$$f_0^{1,\lambda}(x) = x^{\frac{1}{2}|M|} \sum_{n=0}^{n_{max}} a_n x^n, \tag{A.9}$$

where the recurrence relation for the coefficients a_n is:

$$a_{n+2} = -\frac{4\eta_2^n a_n}{(2n+M+4)^2 - M^2}, \tag{A.10}$$

with $n_{\max} = \frac{1}{2}(\lambda - M - 2)$. Therefore λ must be even. The overlap integral is

$$\int_0^1 f_0^{1,\lambda}(x) f_0^{1,\lambda'}(x)(1-x^2)x\,dx = \mathcal{N}_\lambda \delta_{\lambda,\lambda'}. \tag{A.10}$$

$T = 1$, *M odd.* The general solution is written

$$\Phi^{1,M,\lambda}_{T_z}(\Gamma, \phi, \theta_i) = \frac{e^{2iM\phi}}{\sqrt{\pi}} \left\{ (f_1^{1,\lambda}(x) + f_{-1}^{1,\lambda}(x)) \frac{\sin\Gamma}{\sqrt{2}} (\mathscr{D}^1_{T_z,1}(\theta_i) + \mathscr{D}^1_{T_z,-1}(\theta_i)) \right.$$
$$\left. - \cos\Gamma (f_1^{1,\lambda}(x) - f_{-1}^{1,\lambda}(x)) \mathscr{D}^1_{T_z,0}(\theta_i) \right\}. \tag{A.11}$$

The two functions $f_1^{1,\lambda}$ and $f_{-1}^{1,\lambda}$ satisfy the coupled equations:

$$\left\{ (1-x^2)\frac{d^2}{dx^2} + \frac{1-4x^2}{x}\frac{d}{dx} - \left[\frac{(M-1)^2}{4x^2} - \frac{\lambda(\lambda+4)-5}{4} \right] \right\} f_1^{1,\lambda}(x)$$
$$- \left\{ \frac{d}{dx} + \frac{M+1}{2x} \right\} f_{-1}^{1,\lambda}(x) = 0,$$
$$\left\{ (1-x^2)\frac{d^2}{dx^2} + \frac{1-4x^2}{x}\frac{d}{dx} - \left[\frac{(M+1)^2}{4x^2} - \frac{\lambda(\lambda+4)-5}{4} \right] \right\} f_{-1}^{1,\lambda}(x)$$
$$- \left\{ \frac{d}{dx} - \frac{M-1}{2x} \right\} f_1^{1,\lambda}(x) = 0. \tag{A.12}$$

Only the cases $M > 0$ need to be considered (the cases $M < 0$ correspond to an interchange of $f_1^{1,\lambda}$ and $f_{-1}^{1,\lambda}$). The solutions of (A.12) are

$$f_1^{1,\lambda}(x) = x^{\frac{1}{2}(M-1)} \sum_{n=0}^{n_{\max}} a_n x^n, \qquad f_{-1}^{1,\lambda}(x) = x^{\frac{1}{2}(M+1)} \sum_{n=0}^{n_{\max}} b_n x^n. \tag{A.13}$$

The recurrence relations for their coefficients are

$$a_{n+4}(n+2)(n+4)(n+M+1)(n+M+3)$$
$$+ a_{n+2}(n+2)(n+M+1)(\eta_4^n + \eta_2^n - 1) + a_n \eta_2^n \eta_0^n = 0,$$
$$b_n = \frac{\eta_0^n}{n+M+1} a_n + (n+2)a_{n+2}. \tag{A.14}$$

The overlap integral is

$$\int_0^1 \{ (f_1^{1,\lambda} f_1^{1,\lambda'} + f_{-1}^{1,\lambda} f_{-1}^{1,\lambda'}) - x(f_1^{1,\lambda} f_{-1}^{1,\lambda'} + f_1^{1,\lambda'} f_{-1}^{1,\lambda}) \} x\,dx = \mathcal{N}_\lambda \delta_{\lambda\lambda'}. \tag{A.15}$$

$T = 2$, M *even*. The general solution is written

$$\Phi^{2,M,\lambda}_{T_z}(\Gamma, \phi, \theta_i) = \frac{e^{2iM\phi}}{\sqrt{\pi}}$$
$$\times \{\sqrt{\tfrac{2}{3}}[\cos^2 \Gamma(f_0^{2,\lambda} + f_2^{2,\lambda} + f_{-2}^{2,\lambda}) + \tfrac{1}{2}\sin^2 \Gamma(-f_0^{2,\lambda} + f_2^{2,\lambda} + f_{-2}^{2,\lambda})]\mathscr{D}^2_{T_z,0}(\theta_i)$$
$$+ \tfrac{1}{2}\sin 2\Gamma(f_{-2}^{2,\lambda} - f_2^{2,\lambda})(\mathscr{D}^2_{T_z,1}(\theta_i) + \mathscr{D}^2_{T_z,-1}(\theta_i))$$
$$+ \tfrac{1}{2}\sin^2 \Gamma(-f_0^{2,\lambda} + f_2^{2,\lambda} + f_{-2}^{2,\lambda})(\mathscr{D}^2_{T_z,-2}(\theta_i) + \mathscr{D}^2_{T_z,-2}(\theta_i))\}. \tag{A.16}$$

The three functions $f_0^{2,\lambda}(x)$, $f_2^{2,\lambda}(x)$ and $f_{-2}^{2,\lambda}(x)$ satisfy the coupled system:

$$\left\{(1-x^2)\frac{d^2}{dx^2} + \frac{1-5x^2}{x}\frac{d}{dx} + \frac{\lambda(\lambda+4)}{4} - \frac{M^2}{4x^2} - 3\right\} f_0^{2,\lambda}(x)$$
$$+ \left\{2\frac{d}{dx} - \frac{M-2}{x}\right\} f_2^{2,\lambda} + \left\{2\frac{d}{dx} + \frac{M+2}{x}\right\} f_{-2}^{2,\lambda} = 0,$$

$$\left\{(1-x^2)\frac{d^2}{dx^2} + \frac{1-5x^2}{x}\frac{d}{dx} + \frac{\lambda(\lambda+4)}{4} - \frac{(M-2)^2}{4x^2} - 3\right\} f_2^{2,\lambda} + \left\{\frac{d}{dx} + \frac{M}{2x}\right\} f_0^{2,\lambda} = 0,$$

$$\left\{(1-x^2)\frac{d^2}{dx^2} + \frac{1-5x^2}{x}\frac{d}{dx} + \frac{\lambda(\lambda+4)}{4} - \frac{(M+2)^2}{4x^2} - 3\right\} f_{-2}^{2,\lambda} + \left\{\frac{d}{dx} - \frac{M}{2x}\right\} f_0^{2,\lambda} = 0. \tag{A.17}$$

For $M = 0$, the $K = \pm 1$ and $K = 0, \pm 2$ parts of the wave functions can be decoupled by defining

$$\mathscr{U}_{|K|=1}(x) = f_{-2}^{2,\lambda} - f_2^{2,\lambda}, \qquad \mathscr{V}(x) = f_2^{2,\lambda} + f_{-2}^{2,\lambda}. \tag{A.18}$$

The solutions are, then

$$f_0^{2,\lambda}(x) = \sum_{n=0}^{n_{\max}} a_n x^n, \qquad \mathscr{U}_{|K|=1} = \sum_{n=0}^{n_{\max}} r_n x^{n+1}, \qquad \mathscr{V} = \sum_{n=0}^{n_{\max}} S_n x^{n+1}. \tag{A.19}$$

The recurrence relations for the coefficients are

$$r_{n+2} = -\frac{\eta_4^n r_n}{(n+2)(n+4)}, \qquad |K| = 1, \tag{A.20}$$

$$\left.\begin{aligned} &(n+2)^2(n+4)^2 a_{n+4} + (n+2)^2[\eta_6^n + \eta_4^n - 4]a_{n+2} + \eta_2^n \eta_4^n a_n = 0, \\ &S_n = -\frac{1}{2}\frac{\eta_2^n}{n+2} a_n - \tfrac{1}{2}(n+2)a_{n+2}, \end{aligned}\right\} |K| = 0, 2.$$

For $M \neq 0$ (only $M > 0$ need to be considered) the solutions can be written

$$f_0^{2,\lambda}(x) = x^{\frac{1}{2}M} \sum_{n=0}^{n_{\max}} a_n x^n, \qquad f_2^{2,\lambda}(x) = x^{\frac{1}{2}(M+2)} \sum_{n=0}^{n_{\max}} b_n x^n, \qquad f_{-2}^{2,\lambda}(x) = x^{\frac{1}{2}(M-2)} \sum_{n=0}^{n_{\max}} c_n x^n. \tag{A.21}$$

The corresponding recurrence relations for their coefficients are

$$a_n = -\frac{\eta_0^n}{(n+M)} b_n - (n+2)b_{n+2},$$

$$c_n = \frac{\eta_0^n \eta_2^n b_n}{2(n+M)(n+M+2)} + \frac{(n+2)}{2(n+M+2)}(\eta_2^n + \eta_0^n - 2)b_{n+2} + \tfrac{1}{2}(n+2)(n+4)b_{n+4},$$

$$\begin{aligned} 0 = {} & \eta_4^n \eta_2^n \eta_0^n b_n + (n+2)(n+M)\eta_4^n(\eta_2^n + \eta_4^n + \eta_6^n - 4)b_{n+2} \\ & + (n+2)(n+4)(n+M)(n+M+2)(\eta_4^n + \eta_6^n + \eta_8^n - 4)b_{n+4} \\ & + (n+2)(n+4)(n+6)(n+M)(n+M+2)(n+M+4)b_{n+6}. \end{aligned} \tag{A.22}$$

The overlap integral is

$$\begin{aligned} \int_0^1 [& f_0^{2,\lambda} f_0^{2,\lambda'} \tfrac{1}{6}(1+3x^2) + \tfrac{1}{3}(3-x^2)(f_2^{2,\lambda} f_2^{2,\lambda'} + f_{-2}^{2,\lambda} f_{-2}^{2,\lambda'}) + \tfrac{2}{3}x^2(f_2^{2,\lambda} f_{-2}^{2,\lambda'} + f_{-2}^{2,\lambda} f_2^{2,\lambda'}) \\ & + \tfrac{2}{3}x\{f_0^{2,\lambda}(f_2^{2,\lambda'} + f_{-2}^{2,\lambda'}) + f_0^{2,\lambda'}(f_2^{2,\lambda} + f_{-2}^{2,\lambda})\}]x\,dx = \mathcal{N}_\lambda \delta_{\lambda,\lambda'}. \end{aligned} \tag{A.23}$$

$T = 2$, M odd. The general solution is written

$$\begin{aligned} \Phi_{T_z}^{2,M,\lambda}(\Gamma, \phi, \theta_i) = {} & \frac{e^{2iM\phi}}{\sqrt{\pi}} \sin 2\Gamma \\ & \times [-\cos\Gamma(f_1^{2,\lambda} - f_{-1}^{2,\lambda})(\mathscr{D}_{T_z,1}^2 - \mathscr{D}_{T_z,-1}^2) + \sin\Gamma(f_1^{2,\lambda} + f_{-1}^{2,\lambda})(\mathscr{D}_{T_z,2}^2 - \mathscr{D}_{T_z,-2}^2)]. \end{aligned} \tag{A.24}$$

Here $f_1^{2,\lambda}(x)$ and $f_{-1}^{2,\lambda}(x)$ satisfy the coupled equations

$$\begin{aligned} & \left\{(1-x^2)\frac{d^2}{dx^2} + \frac{1}{x}(1-6x^2)\frac{d}{dx} + \frac{\lambda(\lambda+4)}{4} - \frac{21}{4} - \frac{(M-1)^2}{4x^2}\right\} f_1^{2,\lambda} \\ & \qquad - \left\{\frac{d}{dx} + \frac{M+1}{2x}\right\} f_{-1}^{2,\lambda} = 0, \\ & \left\{(1-x^2)\frac{d^2}{dx^2} + \frac{1}{x}(1-6x^2)\frac{d}{dx} + \frac{\lambda(\lambda+4)}{4} - \frac{21}{4} - \frac{(M+1)^2}{4x^2}\right\} f_{-1}^{2,\lambda} \\ & \qquad - \left\{\frac{d}{dx} - \frac{M-1}{2x}\right\} f_1^{2,\lambda} = 0. \end{aligned} \tag{A.25}$$

The solutions of (A.25) are

$$f_1^{2,\lambda}(x) = x^{\frac{1}{2}(M-1)} \sum_{n=0}^{n_{\max}} a_n x^n, \qquad f_{-1}^{2,\lambda}(x) = x^{\frac{1}{2}(M+1)} \sum_{n=0}^{n_{\max}} b_n x^n, \tag{A.26}$$

where the coefficients are determined by means of the recurrence relations

$$\begin{aligned} & a_{n+4}(n+2)(n+4)(n+M+1)(n+M+3) + a_{n+2}(n+2)(n+M+1)(\eta_4^n + \eta_6^n - 1) \\ & \qquad + \eta_2^n \eta_4^n a_n = 0, \end{aligned} \tag{A.27}$$

$$b_n = \frac{\eta_2^n a_n}{(n+M+1)} + (n+2)a_{n+2}\,.$$

The overlap integral is

$$\int_0^1 \{(f_1^{2,\lambda} f_1^{2,\lambda'} + f_{-1}^{2,\lambda} f_{-1}^{2,\lambda'}) - x(f_1^{2,\lambda} f_{-1}^{2,\lambda'} + f_{-1}^{2,\lambda} f_1^{2,\lambda'})\} x(1-x^2)dx = \delta_{\lambda\lambda'} \mathcal{N}_\lambda\,.$$

References

1) D. R. Bès, R. A. Broglia, R. P. J. Perazzo and K. Kumar, Nucl. Phys. **A143** (1970) 1
2) G. G. Dussel, R. P. J. Perazzo, D. R. Bès and R. A. Broglia, Nucl. Phys. **A175** (1971) 513
3) A. Bohr, Mat. Fys. Medd. Dan. Vid. Selsk. **26** (1952) no. 14
4) A. Bohr, Proc. Int. Symp. on nuclear structure, Dubna, 1968 (IAEA, Vienna, 1968) p. 179
5) B. Bayman, D. R. Bès and R. A. Broglia, Phys. Rev. Lett. **23** (1969) 1299
6) O. Nathan, Proc. Int. Symp. on nuclear structure, Dubna 1968 (IAEA, Vienna, 1968) p. 191
7) P. M. Morse and H. Feshbach, Methods of theoretical physics (Mc. Graw-Hill, 1953) pp.784–785
8) D. R. Bès, Nucl. Phys. **10** (1959) 373
9) J. Ginocchio and J. Weneser, Phys. Rev. **170** (1968) 859
10) G. G. Dussel, E. E. Maqueda and R. P. J. Perazzo, Nucl. Phys. **A153** (1970) 469
11) G. G. Dussel and D. R. Bès, Nucl. Phys. **A143** (1970) 623
12) O. Dragùn, G. G. Dussel, E. E. Maqueda and R. P. J. Perazzo, Nucl. Phys. **A167** (1971) 529
13) J. Damgaard, private communication;
D. R. Bès, R. A. Broglia and O. Hansen, private communication;
B. Sørensen, Contr. to session II of the Asilomar Conf. on Nuclear Isospin (Academic Press, N.Y., 1969) and private communication